Cement & Concrete Composites 26 (2004) 705–715

Cement & Concrete Composites

www.elsevier.com/locate/cemconcomp

Experimental analysis of coupled water and chloride transport in cement mortar

Robert Černý [a,*], Zbyšek Pavlík [a], Pavla Rovnaníková [b]

[a] *Department of Structural Mechanics, Faculty of Civil Engineering, Czech Technical University, Thákurova 7, 166 29 Prague 6, Czech Republic*

[b] *Institute of Chemistry, Faculty of Civil Engineering, Technical University of Brno, Žižkova 17, 662 37 Brno, Czech Republic*

Received 25 September 2002; accepted 17 June 2003

Abstract

Coupled water and chloride transport in cement mortar is analyzed experimentally in the paper. Samples with initial moisture content corresponding to 45% relative humidity are subjected to one-sided sodium chloride-in-water solution uptake, and moisture profiles and chloride concentration profiles are determined in three chosen time intervals. In the evaluation of measured moisture profiles and chloride concentration profiles, diffusion model is employed. Moisture diffusivity is determined as function of moisture content and chloride diffusion coefficient as function of chloride concentration using two methods commonly used for analysis of moisture profiles, namely the double integration method and the Matano method. The highest values of both coefficients are obtained by Matano method for the curves corresponding to 24 h exposure to the solution, the lowest values by Matano method for 168 h, the results obtained by double integration method are in between. The complementary experiments with distilled water as penetrating liquid performed for the sake of comparison do not show this feature. It is observed that water transport in the initial time period is for the chloride solution faster and in later times slower than for distilled water. Therefore, the observed differences in the calculated apparent values of moisture diffusivity and chloride concentration coefficients are attributed to the fact that Cl^- and Na^+ ions are adsorbed on the pore walls faster than water molecules. This effect should be included into the mathematical models using ion binding isotherms.

Keywords: Water transport; Chloride transport; Diffusion; Experimental analysis

1. Introduction

Service life of steel-reinforced concrete structures is strongly influenced by reinforcement corrosion. The voluminous corrosion products whose molar volume is almost seven times larger than the volume of the original iron are formed that generate pressures on the concrete covering layer, where cracks are formed, and in the final phase, this layer peels off.

The corrosion processes of steel reinforcement have an electrochemical character that requires the presence of electrolyte. In fresh and non-carbonated concrete, the electrolyte has a high concentration of hydroxide ions ($pH \sim 12.5$) produced by cement hydration. Therefore, a protective passive film forms spontaneously on the steel surface. If the concentration of hydroxide ions decreases under $pH \sim 9$, and if molecules of water and oxygen are present, the corrosion starts. The corrosion process includes the anodic disolution of iron and cathodic process of oxygen depolarization.

There are several effects that can increase the critical pH value of the electrolyte that is necessary for starting the reinforcement corrosion process. One of the most important is the chloride ion penetration to steel surface through the protecting concrete cover. When a sufficient chloride concentration, a threshold value, is reached on the steel surface, the passivating film disrupts and the corrosion process is started. The corrosion process is in progress even if alkalinity is high. Combination of chloride penetration and concrete carbonation accelerates the process of steel corrosion. Therefore, chloride diffusion is a frequently studied topic in concrete research.

---

[*] Corresponding author. Tel.: +420-2243-54429; fax: +420-2243-10775.

E-mail address: cernyr@fsv.cvut.cz (R. Černý).

0958-9465/$ - see front matter © 2003 Elsevier Ltd. All rights reserved.
doi:10.1016/S0958-9465(03)00102-1

Most of the applied models are very simple, and employ 1-D Fick's diffusion equation for the chloride concentration with constant diffusion coefficient and constant initial and boundary conditions,

$$\frac{\partial C}{\partial t} = D\frac{\partial^2 C}{\partial x^2}, \tag{1}$$

$$C(0,t) = C_0, \tag{2}$$

$$C(\infty,t) = 0, \tag{3}$$

$$C(x,0) = 0, \tag{4}$$

where D is the diffusion coefficient; C, the chloride concentration; C_0, the chloride concentration at the exposed boundary; x, the distance from the exposed boundary; t, the time.

The problem (1)–(4) has a very simple mathematical solution (e.g., [1]):

$$C(x,t) = C_0\left[1 - \mathrm{erf}\left(\frac{x}{2\sqrt{Dt}}\right)\right], \tag{5}$$

and this is the main reason for its high application frequency. This model was employed for instance by Tuutti [2], Funahashi [3], Cady and Weyers [4], Weyers [5], Zemajtis et al. [6], Costa and Appleton [7] and many others. Some of the authors, for example Zemajtis et al. [6], assume the surface concentration as a function of the square root of time, or in more general form (e.g., [7]) as a power function of time,

$$C_0(t) = C_1 t^n, \tag{6}$$

where C_1 is the surface chloride concentration after one year, t is expressed in years, and n is an empirical coefficient.

The main weaknesses of these models are the assumption of the constant diffusion coefficient and the fact that they neglect the influence of water transport on the transport of chemical compounds. As a consequence, a single value of the diffusion coefficient can never be obtained from the measured concentration profiles, particularly if the measurements are performed over longer time periods. The diffusion coefficient then appears as a function of time. Nevertheless, these models proved to be useful in many practical applications because the calculated diffusion coefficients have at least a relative value, i.e. it is possible to compare diffusion coefficients in different types of concrete and different environments.

The most frequently used methods for the determination of salt diffusion coefficients in concrete use the experimental set-up designed for the so-called "Rapid Chloride Permeability Test" (sometimes called as "Migration Test"), which was developed at the beginning of the 1980s in USA [8,9]. The experiment uses two cells separated by a plate specimen of the measured material. In measuring chloride diffusion, cell 1 normally contains a NaCl solution, and cell 2 is filled with a NaOH solution of the same molar concentration as that of the chloride source solution. Two mesh electrodes are fitted, one on each side of the concrete specimen in such a way that the electric field is applied primarily across the test specimen.

After establishing steady-state conditions, the diffusion coefficient can be determined using the Nernst–Planck equation

$$\vec{j}_i = \frac{z_i F}{RT} D_i \rho_i \vec{E}, \tag{7}$$

where j_i is the mass flux (in kg/m^2 s) of the particular ion; z_i, its valence; F, the Faraday constant (96487 C/mol); R, the universal gas constant (8.314 J/mol K); T, the absolute temperature (in K); D_i, the diffusion coefficient; ρ_i, the partial density of the ion i (in kg/m^3); and $\vec{E}$, the electric field intensity.

Taking into account one-dimensional geometry of the experiment, the mass flux j_i can be expressed as

$$j_i = \frac{V_0}{A_0}\frac{\mathrm{d}\rho_i}{\mathrm{d}t}, \tag{8}$$

where V_0 is the volume of the cell; $\frac{\mathrm{d}\rho_i}{\mathrm{d}t}$, the rate of change of partial density of the particular ion in the cell determined using measured change of concentration; and A_0, the surface area of the specimen that is in contact with the solution in the cell (i.e. the cross-section of the specimen). The electric field intensity can be expressed as

$$E = \frac{\Delta\varphi}{L}, \tag{9}$$

where $\Delta\varphi$ is the potential difference between the two electrodes; L, the thickness of the specimen. Substituting Eq. (9) into Eq. (7), we obtain

$$D_i = \frac{j_i RTL}{z_i F \rho_i \Delta\varphi}. \tag{10}$$

The above treatment for the determination of the salt diffusion coefficient (described by Andrade et al. [10] or Zhang and Gjørv [11]) can be applied by assuming the following simplifications [12]. First, the ionic mobility is much higher in the solution than in the concrete specimen. Therefore, the "distance" of the experiment is the specimen thickness. Second, mass transport by convection is negligible. Third, classical Fick's diffusion is not considered because its influence is negligible compared to the migration term. This is due to the high value of the expression $\frac{z_i F}{RT}$ when multiplied by the applied potential difference (usually higher than 10 V). Finally, the electric field along the concrete specimen follows a linear course.

These assumptions are relatively strong. Hence, the reliability of "Migration Tests" is often discussed in the scientific literature. A direct comparison with the classical Ficks's diffusion test, which was carried out under identical experimental arrangements as the "Accelerated Diffusion Test" described before (apart from the application of electric field), has shown [13], that the diffusion coefficient values from the "Conventional Diffusion Test" were systematically lower than those of "Accelerated Diffusion Test", typically by a factor difference of about 1.6–2.2.

It should be noted [10] that the duration of the "Accelerated Diffusion Test" is significantly longer than the classical "Rapid Chloride Permeability Test". Typically one week may be enough for ordinary concretes with specimens 1 cm thick. Nevertheless, the test is significantly shorter compared to the "Conventional Diffusion Test", which may take several months.

Another possibility for determining the salt diffusion coefficient is to use a mathematical analysis of measured salt profiles. A typical experiment for the determination of the salt profile in a concrete specimen was described by Baroghel-Bouny et al. [14] for chloride penetration. Concrete samples cured in wet conditions were exposed to a chloride solution from one side in a one-dimensional transport arrangement. After a specified time, slices 3–4 mm thick were cut in the near-surface layer for chloride analysis. The total chloride content was extracted from the specimens using a boiling nitric acid solution for 30 min. The free chloride content was determined after a contact time of 3 min between water and concrete. Chloride concentrations were measured by potentiometry using a titrated silver nitrate solution.

The mathematical analysis of experimentally determined salt profiles depends on the assumed mode of salt transport in the material. If purely diffusion transport is assumed, common methods for solving the inverse problems for parabolic equations can be used.

The simplest method makes the assumption that the diffusion coefficient is constant, the domain under solution is semi-infinite, and the boundary condition on the remaining side of a one-dimensional arrangement is Dirichlet-type. Then diffusion coefficient can be identified using the simple analytical solution of the parabolic problem with error function (5). This method was employed for chloride diffusion for example by Baroghel-Bouny et al. [14].

The dependence of the diffusion coefficient on salt concentration can be found if some more sophisticated methods for the analysis of measured salt profiles are used. However, such methods are not yet commonly used in analyzing salt profiles. One of the few exceptions is the work by Tumidajski et al. [15], where a classical Boltzmann–Matano analysis was employed to determine chloride diffusion coefficients.

In this paper, an analysis of coupled water and chloride transport in concrete is done. During a single experiment in the conditions of one-sided chloride-in-water solution uptake, both chloride diffusion coefficients in dependence on chloride concentration and moisture diffusivities in dependence on moisture content are determined for several cement mortars. For the sake of comparison, moisture diffusivity is also measured for distilled water in otherwise the same conditions.

2. Determination of diffusion coefficients

If only diffusion mode of salt transport is assumed, the calculation of concentration-dependent diffusion coefficients from the measured salt profiles can be done using similar inverse methods as those for the determination of moisture-dependent moisture diffusivity or temperature-dependent thermal conductivity.

On the basis of the previous experience with the solution of inverse problems of moisture diffusion and heat conduction (for a detailed analysis see [15]) we will employ two methods for determination of the $D(C)$ function in this paper, namely the Matano method (originally for diffusion in metals Matano [16], for moisture diffusion then e.g. [17]), which is most frequently used in the inverse analysis of moisture profiles, and the double integration method (for moisture diffusion [17], for heat conduction [18]), which was in the previous work shown as the most reliable (see the error analysis in [19]).

As the basic ideas of the methods are the same as in the above sources and only slight modifications are necessary to adjust the methods directly to the salt diffusion problem, the derivation of both mentioned methods is shown in Appendix A.

3. Materials and samples

In the experimental work, the samples of cement mortar were used. The composition of the mixture of cement mortar for one charge was the following: Portland cement—450 g (three types of cement were applied for different sample groups, namely CEM I 42.5 R Lafarge, CEM I 52.5 R Lafarge and CEM I 42.5 R Prachovice), natural quartz sand with continuous granulometry I, II, III (the total screen residue on 1.6 mm 2%, on 1.0 mm 35%, on 0.50 mm 66%, on 0.16 mm 85%, on 0.08 mm 99.3%—according to the Czech standard ČSN 72 1208)—1350 g, water—225 g. The mixture was put into $40\times40\times160$ mm moulds and compacted by 10 impacts of the compactor. After one day the samples were unmoulded and stored in a 100% relative humidity environment for 27 days. Then, the samples were dried, left for several weeks freely in the laboratory (relative humidity 45%, temperature between 20 and 22 °C) so that they achieved equilibrium moisture content. Finally, all their edges were water and vapor-proof insulated by an epoxy varnish.

4. Experimental results and discussion

The organization of the experiments was the same as in common water sorption experiments. The samples were exposed by their 40×40 mm face to the NaCl solution with the concentration of 18.195 g Cl$^-$ in 1 l of the solution. Duration of the experiment was 1, 24 h and 7 days for three different groups of samples. After this time, the samples were cut into eight pieces and in each piece water content and chloride concentration were measured. Moisture content was determined by the gravimetric method using weighing the moist and dried specimens. In the determination of chloride concentration, the particular samples were after drying first ground by a vibration mill so that grains smaller than 0.063 mm were obtained. Then 10 g of the ground sample was leached 30 min in 180 ml of 80 °C warm distilled water, a magnetic stirrer was used to speed up the leaching process. The content of chlorides in the leach was determined by a turbidity method, i.e. titration of the volumetric solution of mercuric nitrate on the sodium nitroprusside indicator. The first turbidity indicated the equivalence point. On the basis of consumption of mercuric nitrate, the content of water-soluble chlorides in the sample was determined and related to the mass of the hardened mortar.

Figs. 1 and 2 show typical chloride concentration profiles in % (kg of Cl$^-$ per kg of the dry porous body) and moisture profiles in % (kg of water per kg of the dry porous body). The profiles for other types of cement used were qualitatively very similar.

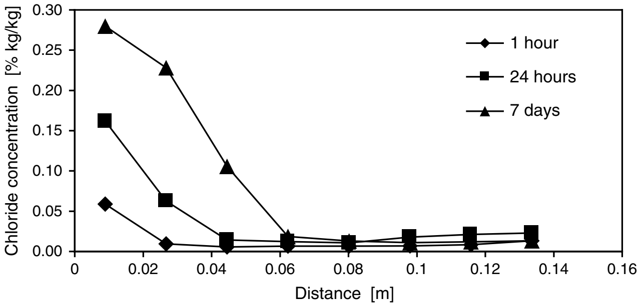

Fig. 1. Chloride concentration profiles—CEM I 42.5 R Lafarge.

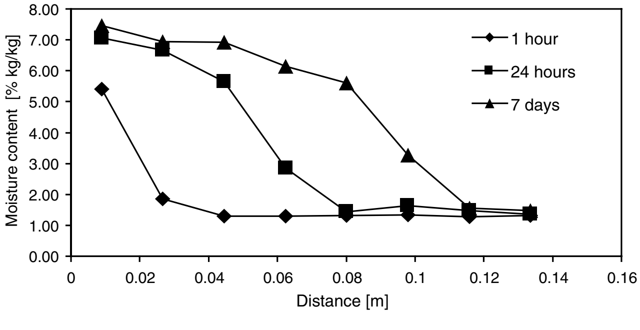

Fig. 2. Moisture profiles—CEM I 42.5 R Lafarge.

There are three interesting features observed on the measured profiles that should be mentioned before further analysis. First is the fact that both chloride concentration profiles and moisture profiles exhibit nonzero values even for the lowest measurement time of 1 h. For moisture profiles this is not very surprising. The initial moisture content in the samples has to correspond to the conditions in the laboratory where they were left for several weeks (45% relative humidity environment). However, the non-zero chloride concentrations deserve a more detailed explanation.

According to Czech standards, any type of cement can contain a maximum of 0.1% of Cl$^-$ by mass. In our case, a leaching experiment on a reference sample not exposed to chloride-in-water solution showed a concentration of 100 mg Cl$^-$ per 1 kg of the mortar, i.e. 0.01% by mass. This meets the requirements of Czech standards. The value of 0.01% of Cl$^-$ by mass also roughly corresponds to the values of chloride concentration measured in the parts of the samples not affected by the approaching water penetration front. The differences from this value are very low and within the error range of the measuring method.

This observation basically means that water dissolved the chlorides originally presented in cement and transported them to the surface of the pores where they either remained dissolved in the surface phase of water or were bound to the pore walls by van der Waals bonds.

The second feature observed by a comparison of Figs. 1 and 2 is that water penetrated into the specimen much faster than chlorides. This is the most interesting observation in our experiments that, however, requires a more detailed explanation. Therefore, a hypothesis explaining this effect will be formulated later.

Third feature is the fact that measured chloride concentrations close to the surface were after already 24 h of penetration higher than the concentration in the penetrating solution. Most probably, a part of chloride ions was bound on the pore walls of the matrix. This is documented more clearly in Fig. 3 where chloride concentrations in g of Cl$^-$ per 100 g of pore water are given. The relatively high concentrations of Cl$^-$ observed in Fig. 3 in the parts of the samples not affected by the approaching water penetration front are apparently a consequence of the fact that moisture content was here very low and the total amount of Cl$^-$ leached from cement was roughly the same as in the other parts of the sample.

Chloride diffusion coefficients in Fig. 4a and b and moisture diffusivities in Fig. 5a and b calculated by both double integration method and Matano method showed that the effect of used cements on the determined transport coefficients was relatively low in the range of

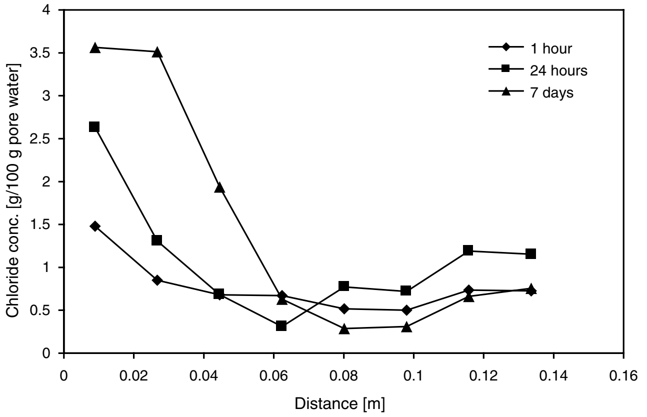

Fig. 3. Chloride concentration profiles, concentration in g of Cl^- per 100 g of pore water—CEM I 42.5 R Lafarge.

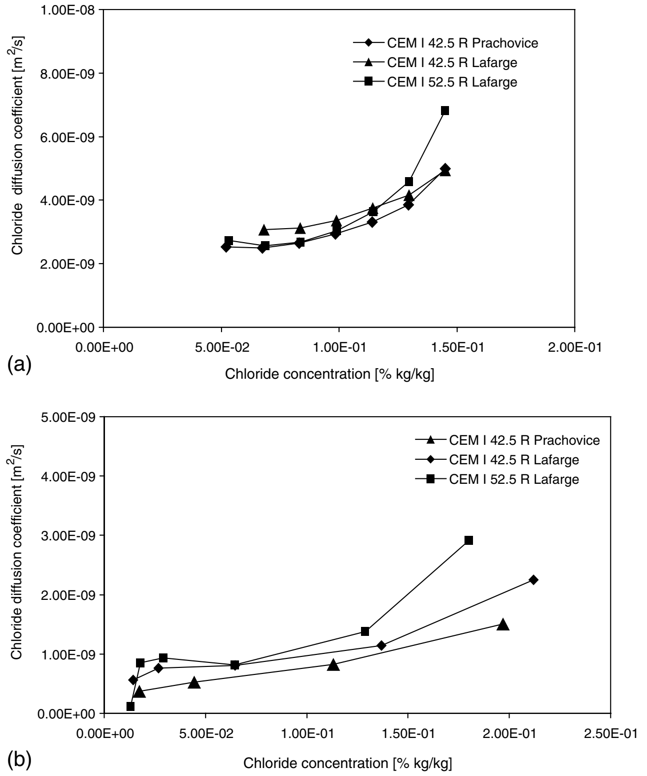

Fig. 4. (a) Chloride diffusion coefficients calculated by the double integration method. (b) Chloride diffusion coefficients calculated by the Matano method, 168 h curve.

low and middle moistures but in the range of higher moisture content the differences were higher.

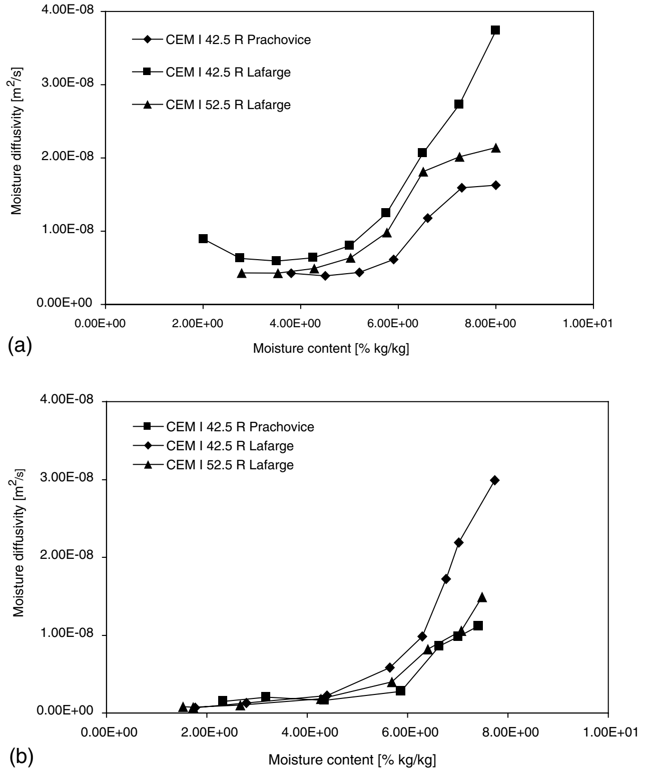

Fig. 5. (a) Moisture diffusivity calculated by the double integration method. (b) Moisture diffusivity calculated by the Matano method, 168 h curve.

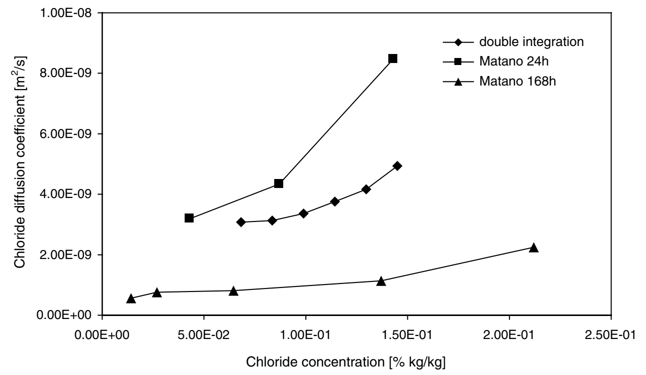

Fig. 6. Chloride diffusion coefficients calculated by different methods—CEM I 42.5 R Lafarge.

Figs. 6 and 7 showed that the differences in the chloride diffusion coefficients and moisture diffusivities calculated by two different methods were significant. Systematically, the highest values of both coefficients were obtained by Matano method for the curves corresponding to 24 h exposure. The lowest values were achieved by calculations using the Matano method for 168 h. The results obtained by double integration method were in between. This result gives an evidence of the time dependence of both chloride diffusion coefficients and moisture diffusivities because the double integration method in the inverse analysis uses all measured profiles at the same time. This effect was observed for all three used cements.

In order to clarify the reasons for the observed differences in the calculated chloride diffusion coefficients and moisture diffusivities, we carried out two verification procedures.

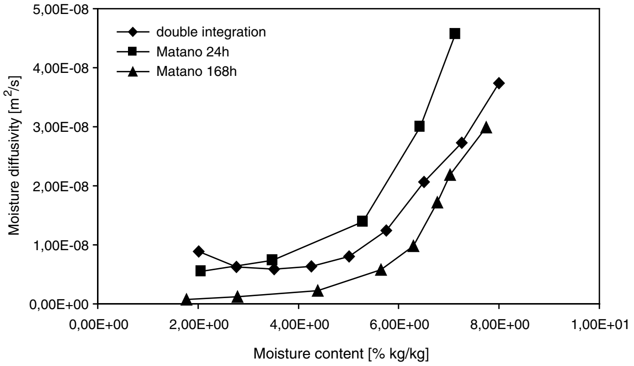

Fig. 7. Moisture diffusivities calculated by different methods—CEM I 42.5 R Lafarge.

The first procedure was numerical. Its aim was to show whether the calculated chloride diffusion coefficients and moisture diffusivities after substitution into the original diffusion equations can reproduce the measured chloride concentration profiles and moisture profiles. In this forward analysis we used the computer code Delphin 4 [20] where we substituted the calculated chloride diffusion coefficients as functions of chloride concentration and moisture diffusivities as functions of moisture content in the form of pointwise given functions.

Fig. 8 shows an example of the verification of results obtained by the Matano method. Both smoothed data for calculation of chloride diffusion coefficient and data calculated using Delphin 4 are given. We can see that data smoothing for calculation of chloride diffusion coefficient was reasonable, and the smoothed curve represented well the measured curve. The calculated curve using Delphin 4 agrees relatively well with the measured curve except for the tail of the curve. However, this is quite logical result because the tails of the chloride concentration curves were not taken into account in calculating diffusion coefficients. Similarly good results were obtained for all chloride diffusion coefficients and moisture diffusivities calculated by the Matano method.

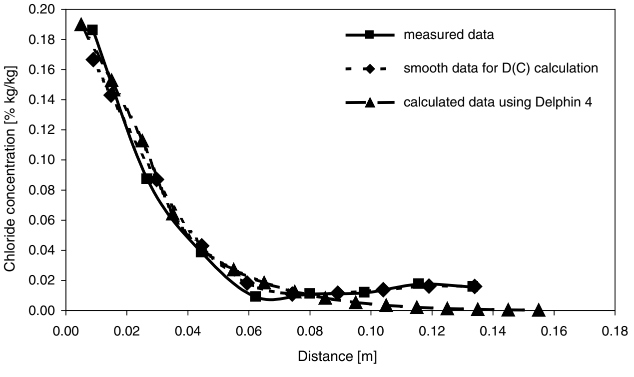

Fig. 8. Comparison of measured and calculated chloride concentration profile for 24 h—CEM I 42.5 R Lafarge, diffusion coefficient determined by the Matano method.

Fig. 9 shows an example of the verification of results obtained by the double integration method. The agreement of measured and calculated chloride concentration profiles is very poor although the smoothed data for calculation of chloride diffusion coefficient agreed well with the measured data (the same smoothing method as in the calculations by Matano method was used). Similarly poor results were obtained for all other calculations.

In solving common moisture transport problems, the main advantage of the double integration method consists in a partial compensation of measuring errors [19] because the method uses some kind of averaging procedure in data processing. For simple moisture transport cases it is very useful particularly for highly split data where the other methods usually fail. In our particular case of coupled moisture and salt transport, this feature of the double integration method resulted in negative effects because the averaging procedure in fact wiped out some real physical–chemical effects.

The second verification procedure was experimental. We carried out an additional set of experiments with distilled water as penetrating liquid but otherwise in the same conditions and again with three different cements. Typical results are presented in Figs. 10 and 11.

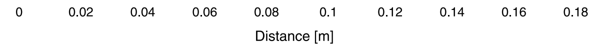

Fig. 9. Comparison of measured and calculated chloride concentration profiles—CEM I 42.5 R Lafarge, diffusion coefficient determined by the double integration method.

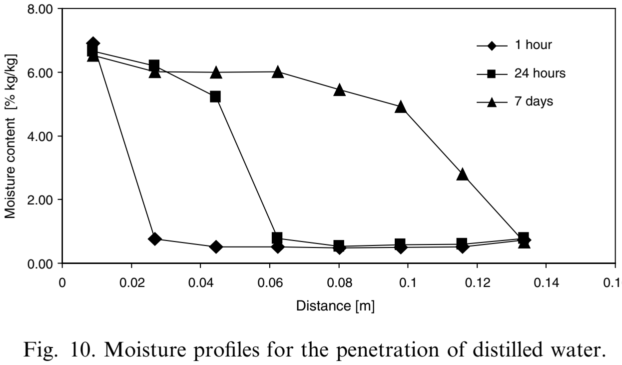

Fig. 10. Moisture profiles for the penetration of distilled water.

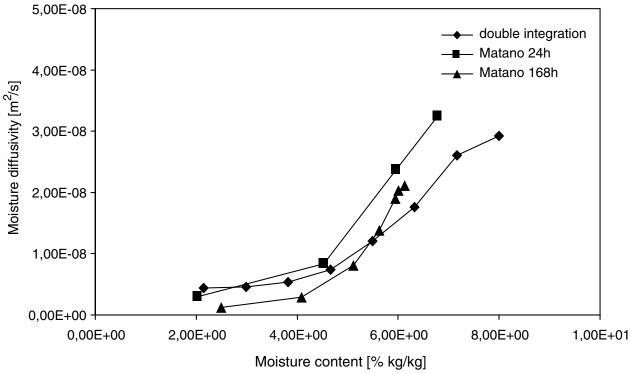

Fig. 11. Moisture diffusivity for the penetration of distilled water.

A comparison of moisture profiles in Figs. 2 and 10 clearly shows that water transport in the case of chloride solution penetration was for the time period of 24 h faster and for the time period of 168 h slower than for the penetration of distilled water. The calculated dependences of moisture diffusivity on the moisture content in Fig. 11 cross each other similarly as in previous measurements with other materials, which is a consequence of usual random errors. No systematic differences as in the case of chloride solution penetration can be observed. Again, the same features were found for all three used cements.

Now, we have the necessary experimental evidence to begin with the explanation of mechanisms of coupled water and chloride transport in cement mortar. However, before we begin, it should be noted that in the evaluation of experiments performed in this paper only apparent chloride diffusion coefficients were determined that in fact include both chlorides in the solution and chlorides fixed on the pore walls. The reason for this form of evaluation was that the chloride binding isotherms were not measured so that the exact amounts of free and bound chlorides could not be distinguished. Another argument why to denote the chloride diffusion coefficients determined in our inverse analysis as "apparent" is the fact that there was simultaneous water and chloride transport in the sample. The inverse analysis then did not include only the motion of chlorides in water but was also affected by the motion of water. The moisture diffusivities determined in our inverse analysis should also be denoted as "apparent" because they are not related to the water itself but to the chloride-in-water solution, i.e. the whole liquid phase.

Taking into account the measurements and calculations in this paper and the preliminary analyses given before, the basic hypothesis for the explanation of mechanisms of coupled water and chloride transport in cement mortar can be formulated as follows.

NaCl represents a classical example of ion bond. It dissociates in water under formation of hydrated ions:

$$\mathrm{NaCl} + \mathrm{H_2O} \rightarrow \mathrm{Na^+(aq)} + \mathrm{Cl^-(aq)}$$

The percentage of ion character IC of the Na–Cl bond can be calculated according to the equation (see [21])

$$\%\mathrm{IC} = \{1 - \exp[-0.25(X_{\mathrm{Na}} - X_{\mathrm{Cl}})^2]\} \times 100 = 55.5,$$

where X_{Na} is the electronegativity of Na, $X_{\mathrm{Na}} = 1.0$; X_{Cl}, the electronegativity of Cl, $X_{\mathrm{Cl}} = 2.8$. This percentage is relatively high and makes very good prerequisites for a formation of van der Waals bonds between the dissociated ions and the molecules of pore walls.

The pore walls in cement-based materials are formed by hydrated calcium silicates and calcium aluminates. Taking into account only silicates, from the difference in electronegativities of silicon and oxygen ($X_{\mathrm{O}} = 3.5$ and $X_{\mathrm{Si}} = 1.7$) it follows that Si–O bond is polar covalent and $\%\mathrm{IC} = 55.5$. Therefore, the adsorption of ions presented in a liquid penetrating into the porous matrix on pore walls based on the formation of van der Waals bonds can be very effective.

Oxygen and hydrogen in water are bonded by covalent bond with a polar character. The polarity of this bond can be expressed using the electronegativities of the particular elements again. As $X_{\mathrm{O}} = 3.5$ and $X_{\mathrm{H}} = 2.2$, we have $\%\mathrm{IC} = 34.5$. The polarity of H–O bond leads on one hand to the formation of hydrogen bond between water molecules. On the other, it also makes possible formation of van der Waals bonds between water molecules and molecules on the pore surface. However, these van der Waals bonds will be weaker than those of dissociated $\mathrm{Cl^-}$ and $\mathrm{Na^+}$ ions. Water molecules have lower partial charges than the almost free $\mathrm{Cl^-}$ and $\mathrm{Na^+}$ ions in the solution. In addition, water has lower bonding capacity due to the fact that water molecules are chained by hydrogen bonds. Therefore, $\mathrm{Cl^-}$ and $\mathrm{Na^+}$ ions can be adsorbed on the pore walls faster than water molecules.

Due to the fast adsorption of $\mathrm{Cl^-}$ and $\mathrm{Na^+}$ ions on pore walls, a part of chloride molecules is immobilized so that it cannot further take part in transport processes in the solution. As a consequence, the apparent transport parameters are lower. This effect can be described in more advanced phenomenological models by using ion binding isotherm as a storage parameter of salt transport (see [15], for more details).

On the other hand, the consequence of adsorption of $\mathrm{Cl^-}$ and $\mathrm{Na^+}$ ions on pore walls is that water molecules cannot be adsorbed on pore walls in such extent as in usual situation when chloride ions are not present. A part of potential van der Waals bonds on the walls is already blocked by chloride ions. Therefore, water molecules are transported by faster capillary forces in higher extent than usually and the apparent transport coefficients are higher.

However, this effect leads after some time to partial separation of water molecules and chloride ions in the solution. Therefore, the solution on the penetration front becomes more dilute and water molecules on the front can again be adsorbed on the pore walls easier. It is a similar situation now as in the case when no chlorides are dissociated in the solution. As a consequence, transport coefficients of water in the porous medium are lower than in the initial phase. The higher viscosity of chloride solution compared to distilled water begins to play a significant role for the transport rate. The apparent chloride transport coefficients also become lower. They do not include now such high amount of ions fixed on pore walls, and ion transport in the solution begins to prevail. This statement can be supported by the fact that the apparent chloride diffusion coefficients (Fig. 4b) determined for 168 h are for higher concentrations close to the value of diffusion coefficient of NaCl in free water (1.67×10^{-9} m^2/s—see [22]).

In addition to the above described adsorption of Cl^- and Na^+ ions on the pore walls that in our hypothesis was supposed to be the main mechanism explaining the slower chloride transport compared to water transport, there is also another potential effect that theoretically could play a significant role in this respect. This is a possible reaction of chloride ions with aluminate phases of hardened cement paste. However, there are different views on these reactions published in the scientific literature. Even generally accepted conclusions concerning the products of reactions of chloride ions with aluminate phases were not formulated until now. On the basis of an extensive literature survey carried out in this respect, we do not believe that reactions of chloride ions with aluminate phases of hardened cement paste played any significant role in our case. We have the following arguments for this statement.

Glasser [23] showed that the capacitive factor concerning the amount of chlorides that can be bonded by the aluminate phases can easily be determined on the basis of the formula of Friedel's salt $3CaO\,.\,Al_2O_3\,.\,CaCl_2\,.\,10H_2O$ (FS). Assuming the density of hardened cement paste 2300 kg/m^3 and the amount of FS after saturation (in a relation to chlorides) 10%, the maximum amount of bonded chlorides could be 29 mg/cm^3. The amount of 10% of FS could seem to be too high but it should be taken into account that also ettringite could be converted into FS. So, the whole or almost whole aluminate phase is potentially available for the formation of $3CaO\,.\,Al_2O_3\,.\,CaCl_2\,.\,10H_2O$.

On the other hand, Taylor [24] stated that during C_3A a C_3S hydration in the presence of gypsum and $CaCl_2$, $3CaO\,.\,Al_2O_3\,.\,CaCl_2\,.\,10H_2O$ was formed not until the whole gypsum was consumed. If NaCl was added to the mixture, 85–98% of the total chloride amount remained in the pore solution of cement paste cured for the time period of 35–70 days. This statement was also supported by several other independent experimental findings quoted in [24] that chlorides are during penetration into concrete partially bonded in Friedel's salt but a large amount of them remains in the solution. At high concentrations of Cl^- ions (typically 8 mol/l), basic components are formed, particularly $3Ca(OH)_2\,.\,CaCl_2\,.\,15H_2O$ [24]. This compound is well soluble in water. Therefore, in the solutions with low Cl^- concentration it was not detected.

Even if we admit that a part of chlorides is bonded into $3CaO\,.\,Al_2O_3\,.\,CaCl_2\,.\,10H_2O$, this amount will not be significant. This statement can be proved very easily. In common Portland cements, C_3A amounts 7–15%. From the total amount of calcium aluminate hydrates, only a small part is located on the pore walls when it can come into contact with chloride ions. The short time of contact (1 h–7 days) is not sufficient for the reaction, particularly taking into account that in the beginning most of chlorides are non-reacted and contained in the pore solution. Basic salts such as $3Ca(OH)_2\,.\,CaCl_2\,.\,15H_2O$ cannot be stable in an environment with a concentration of chloride ions as low as 0.51 mol/l as in our case. Therefore, the explanation based on electronegativities and van der Waals forces given before in our hypothesis seems to be much more probable.

5. Conclusions

Theoretical and experimental studies of coupled water and salt transport belong still to actual topics in describing transport phenomena in cement-based materials because such descriptions are not yet very frequent in concrete research. In this paper, an attempt towards better understanding of mechanisms driving the coupled water and chloride transport in cement mortar was done.

Simple experiments and simple evaluation methods based on the diffusion model of both water and salt transport were carried out. This type of models is naturally not the only one that can be used for modeling water transport in cement-based materials, and maybe even not the most appropriate one particularly for more complicated transport problems (see [15] for a detailed analysis). However, the simplicity of diffusion models makes it possible to analyze fundamental phenomena, which in more complex models could be more or less hidden, in a very straightforward way.

The analysis performed in this paper has clearly shown that description of chloride transport in cement-based materials should always be done in a combination with water transport. The experiments also confirmed that an application of ion binding isotherms in mathematical models of water and salt transport is an unavoidable condition for a realistic description of processes taking place in the porous medium. Neglecting the effects of water transport in the porous material and chloride ion absorption on the pore walls can lead to a departure from the reality. If oversimplified models neglecting the above phenomena are used anyway, their application should always be done for relative purposes only and bearing in mind that some very important factors were not taken into account.

It should be noted that the analysis in this paper was done for cement mortar without any notable cracks. Transport processes in cracked concrete can be significantly enhanced compared to the samples without any cracks. This was shown for instance for water transport by Aldea et al. [25] and for salt transport by Gerard and Marchand [26]. Therefore, an analysis of coupled water and chloride transport in cracked concrete is a very perspective topic that deserves a more detailed investigation.

Another limitation of experiments carried out in this paper is that they were done for wetting only. Combination of wetting and drying periods strongly affects the concentration profiles. This was shown for instance by Polder and Peelen [27]. Further analysis of the effects of wetting and drying cycles can contribute to better understanding of mechanisms of coupled water and chloride transport in more complicated conditions.

It is the intention of the authors of this paper to continue their work in these directions and to carry out such analyses in the near future.

Acknowledgements

This research has been supported partially by the Ministry of Education of the Czech Republic, under contract MSM:210000003 (first two authors), and partially by the Grant Agency of the Czech Republic, project no. 103/00/0607 (third author).

Appendix A. Derivation of the Matano method and the double integration method

We consider 1-D non-linear diffusion equation

$$\frac{\partial C}{\partial t} = \frac{\partial}{\partial x}\left(D(C)\frac{\partial C}{\partial x}\right), \tag{A.1}$$

with constant boundary and initial conditions in the form:

$$C(0,t) = C_1, \tag{A.2}$$

$$C(\infty,t) = C_2, \tag{A.3}$$

$$C(x,0) = C_2. \tag{A.4}$$

We further assume that the concentration field $C(x,t)$ (C as a partially density in the sense of the theory of mixtures is supposed to be given in kg/m^3) is known from the experimental measurements as well as the initial and boundary conditions of the experiment. Solving an inverse problem means in this particular case the determination of the $D = D(C)$ function using the above data.

In the classical Botzmann–Matano treatment [16], the Boltzmann transformation

$$\eta = \frac{x}{2\sqrt{t}}, \tag{A.5}$$

$$\omega(\eta) = C(x,t) \tag{A.6}$$

is used first. Substituting Eqs. (A.5) and (A.6) into Eqs. (A.1)–(A.4) using the relations

$$\frac{\partial C}{\partial x} = \frac{\mathrm{d}C}{\mathrm{d}\eta}\frac{\partial \eta}{\partial x} = \frac{\mathrm{d}C}{\mathrm{d}\eta}\frac{1}{2\sqrt{t}}, \tag{A.7}$$

$$\frac{\partial C}{\partial t} = \frac{\mathrm{d}C}{\mathrm{d}\eta}\frac{\partial \eta}{\partial t} = \frac{\mathrm{d}C}{\mathrm{d}\eta}\cdot\left(-\frac{x}{4t\sqrt{t}}\right) = \frac{\mathrm{d}C}{\mathrm{d}\eta}\cdot\left(-\frac{\eta}{2t}\right), \tag{A.8}$$

we obtain

$$\frac{\mathrm{d}}{\mathrm{d}\eta}\left(D\frac{\mathrm{d}\omega}{\mathrm{d}\eta}\right) + 2\eta\frac{\mathrm{d}\omega}{\mathrm{d}\eta} = 0, \tag{A.9}$$

$$\omega(0) = C_1, \tag{A.10}$$

$$\omega(+\infty) = C_2. \tag{A.11}$$

In this way, the partial differential equation (A.1) is transformed into the ordinary differential equation (A.9). Assuming now that for a given time $t_0 = \text{const.}$, the concentration field $C(x,t_0)$ is known, the following second transformation can be used:

$$z = \eta \cdot 2\sqrt{t_0}, \tag{A.12}$$

$$C(z) = \omega(\eta). \tag{A.13}$$

Substituting Eqs. (A.12) and (A.13) into Eqs. (A.9)–(A.11) we get

$$\frac{\mathrm{d}}{\mathrm{d}z}\left(D\frac{\mathrm{d}C}{\mathrm{d}z}\right) + \frac{z}{2t_0}\frac{\mathrm{d}C}{\mathrm{d}z} = 0, \tag{A.14}$$

$$C(0) = C_1, \tag{A.15}$$

$$C(+\infty) = C_2. \tag{A.16}$$

In solving the system (A.14)–(A.16), we first integrate Eq. (A.14) from the chosen point $z = z_0$ to $z \to \infty$, so that we obtain

$$\left[D\frac{\mathrm{d}C}{\mathrm{d}z}\right]_{z_0}^{\infty} + \frac{1}{2t_0}\int_{z_0}^{\infty} z\frac{\mathrm{d}C}{\mathrm{d}z}\,\mathrm{d}z = 0. \tag{A.17}$$

For $z \to \infty$ we assume a zero value of mass flux (the point is far enough from the salt solution source and at the initial concentration),

$$j_C \to 0, \tag{A.18}$$

and therefore

$$D\frac{\mathrm{d}C}{\mathrm{d}z} \to 0. \tag{A.19}$$

Eq. (A.17) is then modified into the form

$$D(C_0) = \frac{1}{2t_0\left(\frac{\mathrm{d}C}{\mathrm{d}z}\right)_{z=z_0}}\int_{z_0}^{\infty} z\frac{\mathrm{d}C}{\mathrm{d}z}\,\mathrm{d}z, \tag{A.20}$$

where $C_0 = C(z_0, t_0)$. The integral in Eq. (A.20) is solved by common numerical methods, such as Simpson's rule.

Contrary to the Matano method that is in principle a one-curve method, the double integration method by Drchalová and Černý [17] belongs to multiple-curves methods. We assume, that n curves $C(x,t)$ are known from concentration measurements, and again solve the system (A.1)–(A.4), where in (A.3) we have the length of the one-dimensional domain l instead of the semi-infinite domain with $+\infty$. In the solution to the defined inverse problem, we suppose $C(t)$ and $C(x)$ to be monotonic functions, and first choose a constant value of concentration, $\tau = C(x,t)$. There must then exist one-to-one parametrizations $x = x_0(\tau,t)$, $t = t_0(\tau,x)$, where both x_0 and t_0 are monotonic functions. In other words, on the above assumptions it is possible to express x as a function of the chosen concentration τ and time t, and t as a function of τ and position x. The construction of the $\tau = C(x,t)$ curve in the (x,t) plane, i.e. the derivation of the shape of the integration region, is as follows. We choose a time t_A, $t_1 \leqslant t_A \leqslant t_n$, and using an interpolation procedure on the system of measured concentration curves $C(x,t_i)$, $i = 1,2,\ldots,n$, we find the corresponding position x_A for concentration τ. The point $A = [x_A, t_A]$ lies on the boundary of the integration region. Then we choose a sufficient number of other points t_j from the interval $\langle t_1, t_2\rangle$, and in this way we obtain a pointwise function $x = x_0(\tau,t)$, which forms the boundary of the integration region. We now integrate the diffusion equation (A.1) over x and t on the integration region we just have found,

$$\begin{aligned}&\int_{t_1}^{t_n}\int_0^{x_0(\tau,t)} \frac{\partial C}{\partial t}\,\mathrm{d}x\,\mathrm{d}t\\ &\quad = D(\tau)\int_{t_1}^{t_n} \frac{\partial C}{\partial x}(x_0(\tau,t),t)\,\mathrm{d}t - \int_{t_1}^{t_n} D[C(0,t)]\frac{\partial C}{\partial x}(0,t)\,\mathrm{d}t.\end{aligned} \tag{A.21}$$

The left side of Eq. (A.21) would be difficult to solve directly. Therefore, we change the sequence of integration, accounting for the shape of the integration area,

$$\begin{aligned}\mathrm{LS} &= \int_{t_1}^{t_n}\int_0^{x_0(\tau,t)} \frac{\partial C}{\partial t}\,\mathrm{d}x\,\mathrm{d}t\\ &= \int_0^{x_0(\tau,t)} \mathrm{d}x \int_{t_1}^{t_n} \frac{\partial C}{\partial t}\,\mathrm{d}t + \int_{x_0(\tau,t_1)}^{x_0(\tau,t_n)} \mathrm{d}x \int_{t_0(\tau,x)}^{t_n} \frac{\partial C}{\partial t}\,\mathrm{d}t.\end{aligned} \tag{A.22}$$

Denoting

$$\int \frac{\partial C}{\partial t}\,\mathrm{d}t = \int \mathrm{d}C = I_C(C), \tag{A.23}$$

we obtain

$$\begin{aligned}\mathrm{LS} &= \int_0^{x_0(\tau,t_1)} [I_C(C(x,t_n)) - I_C(C(x,t_1))]\,\mathrm{d}x\\ &\quad + \int_{x_0(\tau,t_1)}^{x_0(\tau,t_n)} [I_C(C(x,t_n)) - I_C(\tau)]\,\mathrm{d}x\\ &= \int_0^{x_0(\tau,t_n)} I_C(C(x,t_n))\,\mathrm{d}x - \int_0^{x_0(\tau,t_1)} I_C(C(x,t_1))\,\mathrm{d}x\\ &\quad - I_C(\tau)[x_0(\tau,t_n) - x_0(\tau,t_1)].\end{aligned} \tag{A.24}$$

Taking into account that

$$-D[C(0,t)]\frac{\partial C}{\partial x}(0,t) = j_C(0,t), \tag{A.25}$$

and substituting Eqs. (A.24) and (A.25) into Eq. (A.21), we get

$$\begin{aligned}D(\tau) &= \frac{1}{\int_{t_1}^{t_n} \frac{\partial C}{\partial x}(x_0(\tau,t),t\,\mathrm{d}t}\\ &\quad \times \left(\int_0^{x_0(\tau,t_n)} I_C(C(x,t_n))\,\mathrm{d}x - \int_0^{x_0(\tau,t_1)} I_C(C(x,t_1))\,\mathrm{d}x\right.\\ &\quad \left. - I_C(\tau)[x_0(\tau,t_n) - x_0(\tau,t_1)] - \int_{t_1}^{t_n} j_C(0,t)\,\mathrm{d}t\right),\end{aligned} \tag{A.26}$$

where $j_C(0,t)$ can be determined as

$$j_C\left(0, \frac{t_j + t_i}{2}\right) = \frac{1}{t_j - t_i}\int_0^l [C(x,t_j) - C(x,t_i)]\,\mathrm{d}x. \tag{A.27}$$

References

[1] Carslaw HS, Jaeger JC. Conduction of heat in solids. Oxford: Clarendon Press; 1959.

[2] Tuuti K. Corosion of steel in concrete. Stockholm: Swedish Cement and Concrete Research Institute; 1982.

[3] Funahashi M. Predicting corrosion-free service life of a concrete structure in a chloride environment. ACI Mater J 1982;87:581–7.

[4] Cady PD, Weyers RE. Predicting service life of concrete bridge decks subject to reinforcement corrosion. In: Corrosion forms and control for infrastructure. ASTM STP 1137. American Society for Testing and Materials; 1992. p. 328–38.

[5] Weyers RE. Service life model for concrete structures in chloride laden environments. ACI Mater J 1998;95:445–53.

[6] Zemajtis J, Weyers RE, Sprinkel MM. Corrosion protection service life of low-permeable concretes and low-permeable concrete with a corrosion inhibitor. Transportation Research Report 1642. Washington: National Research Council; 1998. p. 51–9.

[7] Costa A, Appleton J. Chloride penetration into concrete in marine environment. Part II: Prediction of long term chloride penetration. Mater Struct 1999;32:354–9.

[8] Whiting D. Rapid determination of the chloride permeability of concrete. Report No. FHWA/RD-81/119. Portland Cement Association, NTIS DB No. 82140724, 1981.

[9] AASHTO Designation T277-83. Standard method of test for resistance of concrete to chloride ion penetration. Washington, DC: American Association of State Highway and Transportation Officials; 1983.

[10] Andrade C, Castellote M, Cervigon D, Alonso C. Fundamentals of migration experiments. In: Proceedings of the RILEM Inter-

national Workshop Chloride Penetration into Concrete. St-Remy-les-Chevrouse; 1997. p. 95–114.

[11] Zhang T, Gjørv OE. An electrochemical method for accelerated testing of chloride diffusivity in concrete. In: Proceedings of the RILEM International Workshop Chloride Penetration into Concrete. St-Remy-les-Chevreuse; 1997. p. 105–114.

[12] Andrade C. Calculation of chloride diffusion coefficients in concrete from ionic migration experiments. Cem Concr Res 1993;23:724–42.

[13] Arsenault J, Bigas JP, Ollivier JP. Determination of chloride diffusion coefficient using two different steady-state method: influence of concentration gradient. In: Proceedings of the RILEM International Workshop Chloride Penetration into Concrete. St-Remy-les-Chevreuse; 1997. p. 150–60.

[14] Baroghel-Bouny V, Chaussadent T, Raharinaivo A. Experimental investigations on binding of chloride and combined effects of moisture and chloride in cementitious materials. In: Proceedings of the RILEM International Workshop Chloride Penetration into Concrete. St-Remy-les-Chevreuse; 1997. p. 290–301.

[15] Černý R, Rovnaníková P. Transport processes in concrete. London: Spon Press; 2002.

[16] Matano C. On the relation between the diffusion coefficient and concentration of solid metals. Jpn J Phys 1933;8:109–15.

[17] Drchalová J, Černý R. Non steady-state methods for determining the moisture diffusivity of porous materials. Int Comm Heat Mass Transfer 1998;25:109–16.

[18] Černý R, Toman J. Determination of temperature and moisture dependent of thermal conductivity by solving the inverse problem of heat conduction. In: Proceedings of International Symposium of Moisture Problems in Building Walls. University of Porto; 1995. p. 299–308.

[19] Černý R, Drchalová J, Hošková Š, Toman J. Inverse problems of moisture transport in porous materials. In: Proceedings of Second ECCOMAS Conference on Numerical Methods in Engineering. Chichester: John Wiley and Sons; 1996. p. 664–70.

[20] Grunewald J. DELPHIN 4.1—Documentation. Theoretical Fundamentals. TU Dresden, Dresden, 2000.

[21] Pauling L. The nature of the chemical bond. New York: Cornell University Press; 1960.

[22] Johanesson BF. Diffusion of a mixture of cations and anions dissolved in water. Cem Concr Res 1999;29:1261–70.

[23] Glasser FP. Role of chemical binding in diffusion and mass transport. In: Skalny JP et al., editors. Transport in cement-based materials. Westerville: The American Ceramic Society; 2001. p. 129–54.

[24] Taylor HFW. Cement chemistry. 2nd ed. London: Academic Press; 1992.

[25] Aldea CM, Shah SP, Karr A. Permeability of cracked concrete. Mater Struct 1999;32:370–6.

[26] Gerard B, Marchand J. Influence of cracking on the diffusion properties of cement-based materials. Part I: Influence of continuous cracks on the steady-state regime. Cem Concr Res 2000;30:37–43.

[27] Polder RB, Peelen WHA. Characterisation of chloride transport and reinforcement corrosion in concrete under cyclic wetting and drying by electrical resistivity. Cem Concr Compos 2002;24:427–35.